J. Plasma Physics (1997), *vol.* 57, *part* 2, *pp.* 403–423. Printed in the United Kingdom
© 1997 Cambridge University Press

Arbitrary potential drops between collector and emitter in pure electron diodes

HEIDRUN KOLINSKY and HANS SCHAMEL
Physikalisches Institut, Universität Bayreuth, D-95440 Bayreuth, Germany

(Received 9 October 1995 and in revised form 7 March 1996)

A novel Lagrangian integral formalism is applied to pure electron diodes. Analytical expressions are obtained in terms of the injected current and of the potential drop for two DC states. These two states are either completely transmitted flows or flows with partial reflection at a virtual cathode. Splitting rates and other quantities are presented for arbitrary potentials.

1. Introduction

The theory of planar diodes has kept its fascination since its first appearance at the beginning of this century (Child 1911). Both the wide applicability and the rich dynamical phenomena of these simple models contribute to this. Planar diode models are used to describe low-pressure plasmas in plasma processing (Lieberman and Lichtenberg 1994), for example in the fabrication of very-large-scale (VLSI) circuits (Farouki *et al.* 1990) and in plasma immersion ion implantation (Lieberman and Lichtenberg 1994). Another area of application is to microwave generators, for instance the virtual cathode oscillator (vircator) (Sullivan *et al.* 1987) and the reditron, where the time-dependent virtual cathode solutions turn out to be especially important. However, up to now, a consistent analytical description of the virtual cathode oscillations has been missing.

The variety of nonlinear time-dependent solutions cannot be explored analytically: numerical approaches are essential. Remarkable progress has been made in the case of the Pierce diode (Pierce 1944) with regard to bifurcation scenarios and transitions to chaotic behaviour (Crystal and Kuhn 1985; Godfrey 1987; Lawson 1989*a*, *b*). A predominantly analytical theory of weakly nonlinear oscillations in the form of a three-harmonic approximation was given by Hörhager and Kuhn (1990). In the Pierce diode model a cold electron beam between two grounded plates is neutralized by a fixed ion background.

In this paper a new starting point for describing the physics of a collisionless pure electron diode is chosen, motivated by the success of a Lagrangian formulation that has proven superior to an Eulerian description in cases where the ion dynamics is incorporated in Pierce-like diodes (Schamel and Maslov 1993; Kolinsky and Schamel 1994, 1995). As we shall show in the following, the superiority of the Lagrangian method also holds for a pure electron diode, since it is possible to derive analytical expressions for the space-charge-limited current with arbitrary anode potentials, for the minimum current necessary for the existence of a virtual cathode solution, and for the transmitted current as a function of injected current and of anode potential in the case of virtual cathode formation.

https://doi.org/10.1017/S0022377896004886 Published online by Cambridge University Press

In the theoretical model a beam of electrons with density n_0, velocity v_0 and negligible thermal spread enters the drift space between two grids separated by a distance L. The potential drop V between the two grids is kept constant, and the electrons reaching the collector are completely absorbed. The equilibrium solutions are determined by the charge, the mass of the particles (we use electrons, but the equations can be easily rescaled to other species), the density and velocity of the beam at entrance, as well as by the distance between the two grids and by the applied potential. There exist two classes of equilibrium solutions, one of which exhibits reflected electrons. Both states can coexist for a given potential in a certain interval of the injection current. Hysteresis is found, and the state that is realized depends on the prehistory, i.e. whether the current has been raised or lowered. In the following the solutions are studied analytically in detail. The final results are presented as functions of quantities that can be easily controlled in experiments: the injected electron current and the voltage drop.

It should be noted that Kuznetsov *et al.* (1994) have recently investigated the same theoretical model with a different technique, using (η, ϵ) diagrams for studying Bursian diodes. A numerical shooting method was used for finding the corresponding values of the electric field for a given current and potential. By evaluating the (η, ϵ) diagrams, conclusions could also be drawn about stability. After a rescaling, their results coincide with ours; however, one advantage of our more analytical treatment is that the transmitted current of the electron diode in the virtual cathode regime is given analytically as a function of the injected current and of the potential drop V.

The electron beam is treated as a continuous fluid, which in the case of virtual cathode formation can split itself into two parts, one part streaming back to the injection plane, the other passing to the anode. The electron distribution function is assumed to have zero temperature; therefore the Vlasov equation reduces to the hydrodynamic cold-fluid-equation. The beam moves with a velocity much less than that of light, so that magnetic field and relativistic effects can be ignored. Neither transverse variations nor variations perpendicular to the x direction are allowed for any quantity. Therefore the model is simply electrostatic and one-dimensional.

This simple model has a long tradition. Child (1911) presented the first analysis of space-charge-limited currents for a beam with zero or a small thermal injection velocity. Langmuir (1923) solved the same model with a cathode emitting electrons with a half-Maxwellian velocity distribution. He found a so-called α region with electrons flowing out and back to the cathode, and a β region with electrons flowing just to the anode. The minimum of the potential constitutes the boundary of both regions. High electron injection velocities were treated both theoretically and experimentally by Gill (1925). He observed that there exists a maximum current that can be transmitted across the diode. An increase in the electron current beyond this maximum value leads to a sharp decrease in the anode current to a new lower value. He also observed hysteresis, and found that oscillations occur, accompanied by the formation of a virtual cathode. His analysis correctly predicted the maximum current. Further experiments were carried out by Harries (1936*a*, *b*), and further theoretical work by Salzberg and Haeff (1938), Fay *et al.* (1938) and Strutt and van der Ziel (1938). The results of a number of further investigations have been published since then. For an overview, see Birdsall and Bridges (1966, Chap. 3.02).

Time-dependent nonlinear virtual cathode oscillations have been studied in com-

https://doi.org/10.1017/S0022377896004886 Published online by Cambridge University Press

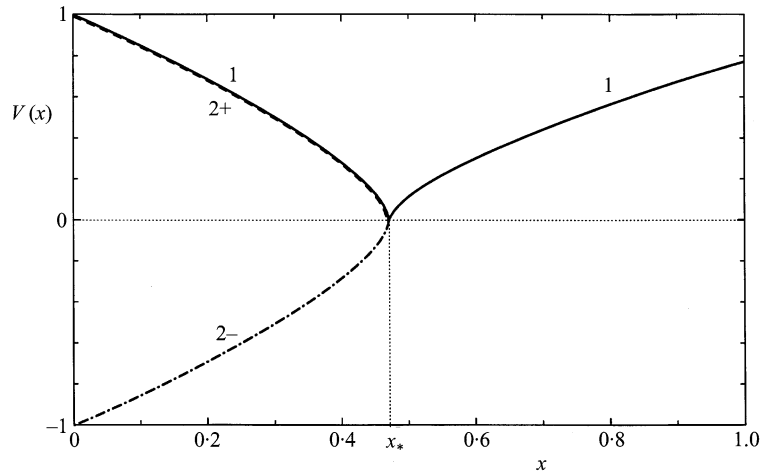


Figure 1. Phase-space portrait for type II flow, with collector potential $V = -0.2$, Pierce parameter $\alpha = 1$, and an equilibrium solution with partial reflection. Subscript 1 denotes the transmitted electron current, 2+ the part of the injected current that is reflected back to the emitter at the virtual cathode, and 2− the beam after reflection. The position of the virtual cathode is denoted by x_*, which depends on V and α.

puter simulations by Dunn and Ho (1963) and Birdsall and Bridges (1966). They reveal that the potential minimum oscillates both in position and height at something like the electron plasma frequency. Coutsias and Sullivan (1983) focused their attention on space-charge limit instabilities of the electron diode, and observed numerically the oscillations of the virtual cathode. They also calculated the nonlinear growth rate for the space-charge-limited current in the short-circuited case.

The outline of this paper is as follows. In Sec. 2 we present the basic equations and the boundary conditions. The Eulerian description is converted into the more suitable Lagrangian description in Sec. 3. The case of no particle reflection is treated for arbitrary potential drops in Sec. 4, where equilibrium solutions are obtained, including a stability analysis. Section 5 is devoted to equilibria with partial reflection of electrons. These equilibria exhibit a virtual cathode, and are realized for injection currents exceeding the space-charge-limited current. In this section a reformulation of quantities such as transmitted current, emitter electric field, transit time and virtual cathode position is performed, leading to new analytical expressions in terms of the injection current and of the potential. Section 6 contains a short summary and conclusions.

2. Basic equations

A three-fluid model is used to describe the motion of the electrons through the diode. The electron beam is split into three parts. Figure 1 shows the phase-space picture. Subscripts are used as follows: 1 denotes the transmitted electrons, 2+ the part of the electron current moving up to the virtual cathode, reaching zero velocity there, and 2− the reflected electron beam. Hence only one electron reflecting barrier is considered. The electron motion is governed by the continuity equations ($i = 1, 2+, 2-$).

$$\partial_t n_i(x,t) + \partial_x \left[n_i(x,t) v_i(x,t) \right] = 0, \tag{1}$$

https://doi.org/10.1017/S0022377896004886 Published online by Cambridge University Press

and by the momentum conservation equation for the electrons

$$\partial_t v_i(x,t) + v_i(x,t)\partial_x v_i(x,t) = -E(x,t). \tag{2}$$

In the electrostatic limit these are coupled by Poisson's equation

$$-\partial_x E(x,t) = \alpha^2 \sum_i n_i(x,t). \tag{3}$$

Normalized quantities are used ($i = 1, 2+, 2-$)

$$\frac{x}{L} \to x', \qquad \frac{n_i}{n_0} \to n_i', \qquad \frac{v_i}{v_0} \to v_i',$$

$$E\frac{eL}{m_e v_0^2} \to E', \qquad t\frac{v_0}{L} \to t', \qquad \frac{q_i}{e} \to q_s' = -1,$$

and primes will be dropped. Thus x denotes the normalized position of the electron fluid element, n_i the normalized density, v_i the velocity, t the time and E the electric field, and the minus sign in (2) results from the electronic charge. The control (Pierce) parameter α is given by

$$\alpha^2 = \frac{n_0 e^2}{\epsilon_0 m_e}\frac{L^2}{v_0^2} = \left(\frac{\omega_{pe}L}{v_0}\right)^2,$$

where n_0 is the electron density at the emitter, v_0 the electron injection velocity, m_e the mass and e the elementary charge. ω_{pe} is the plasma frequency at the cathode. Note that for $x_* < x \leqslant 1$, where x_* is the virtual cathode position, only one electron component exists. The boundary conditions are

$$\begin{aligned} v_1(0,t) &= 1, \\ v_{2+}(0,t) &= 1, \\ \Phi(0,t) &= 0, \\ \Phi(1,t) &= V = -\int_0^1 E(x,t)\,dx. \end{aligned}$$

The density at the cathode is given by

$$n_e(0,t) = n_1(0,t) + n_{2+}(0,t) + n_{2-}(0,t), \tag{4}$$

and $n_{\text{inj}}(0,t) := n_1(0,t) + n_{2+}(0,t)$ is the electron injection density. It is usually kept constant, even in cases of time-dependent dynamics. However, the density of the backstreaming electrons $n_{2-}(0,t)$ will generally be time-dependent, namely in the case of virtual cathode oscillations. Therefore in the non-stationary case $n_e(0,t)$ will be a function of time, and hence so will $\omega_{pe}(t)$ and $\alpha(t)$. This time-dependent case, however, causes serious difficulties, since the electrons return to the position of the emitter and supply a feedback mechanism to the incoming electron beam. Hence we are forced to a further restriction, namely $n_e(0,t) = \text{const}$ in time. As boundary conditions, we therefore use ($\nu = \text{const}$)

$$\begin{aligned} n_1(0,t) &= \nu \quad (0 \leqslant \nu \leqslant 1), \\ n_{2+}(0,t) &= \tfrac{1}{2}(1-\nu), \\ n_{2-}(0,t) &= \tfrac{1}{2}(1-\nu). \end{aligned}$$

This restricted form of the boundary conditions makes it possible to find DC solutions of the following types:

https://doi.org/10.1017/S0022377896004886 Published online by Cambridge University Press

(I) $\nu = 1$, with no particle reflection in the diode region;

(II) $0 < \nu < 1$, with particle reflection with virtual cathode formation and a part of the electrons transmitted to the collector;

(III) $\nu = 0$, with total reflection of the electron beam; this special case demands a different treatment in the analysis, and is not pursued further.

If no electrons are returning to the emitter (type I), a time-dependent perturbation analysis for the steady-state solution can be easily performed. For the steady-state solution of types I and II, a Lagrangian description in the sense of Schamel and Bujarbarua (1993), Schamel and Maslov (1993) and Kolinsky and Schamel (1994, 1995) can be used under the assumption that at least part of the injected electron fluid element reaches the anode, ensuring that $t_0 = t_0(x,t)$ is invertible, so that there exists a unique relation $x(t_0,t)$.

3. Lagrangian formulation

We define

$$t_0(x,t) = t - \frac{1}{\nu}\int_0^x n_1(x',t)\,dx'. \tag{5}$$

This quantity is conserved on the path of fluid element 1 on its way through the diode, and is therefore a 'stream function'. The substantial derivative of t_0 vanishes:

$$\frac{d}{dt}t_0(x,t) = [\partial_t + v_1(x,t)\partial_x]\,t_0(x,t) = 0.$$

Hence t_0 is a Lagrangian variable, labels each element of fluid 1 and corresponds to the entrance time into the diode. Starting from the identity $x = x\,[t_0(x,t),t]$, it then follows that

$$x'(t_0,t) = -\frac{\nu}{\tilde{n}_1(t_0,t)}, \tag{6}$$

$$\dot{x}(t_0,t) = \tilde{v}_1(t_0,t), \tag{7}$$

where $\tilde{f}(t_0,t) \equiv f[x(t_0,t),t]$ holds identically. The Lagrangian quantities are denoted henceforth by a tilde ($\tilde{}$).

Switching from the Eulerian space (x,t) to the Lagrangian space (t_0,t), the differentials are transformed through

$$\partial_x \;\rightarrow\; -\frac{1}{\nu}\tilde{n}_1\partial_{t_0}, \tag{8}$$

$$\partial_t \;\rightarrow\; \partial_t + \frac{1}{\nu}\tilde{n}_1\tilde{v}_1\partial_{t_0}. \tag{9}$$

From (6) and (7) and from the definition (5), it follows that the continuity equation of fluid 1 is automatically satisfied. The momentum equation for fluid 1 leads to

$$\ddot{x}(t_0,t) = -\tilde{E}(t_0,t),$$

and the continuity and momentum equations for both fluids 2+ and 2− can be rewritten as

$$\Xi(t_0,t)\,\tilde{n}_2(t_0,t) = -\partial_{t_0}[\tilde{n}_2(t_0,t)\,\tilde{v}_2(t_0,t)], \tag{10}$$

$$\Xi(t_0,t)\,\tilde{v}_2(t_0,t) = -x'(t_0,t)\tilde{E}(t_0,t) - \tfrac{1}{2}\partial_{t_0}[\tilde{v}_2(t_0,t)]^2, \tag{11}$$

https://doi.org/10.1017/S0022377896004886 Published online by Cambridge University Press

with the operator $\Xi(t_0,t) \equiv x'(t_0,t)\partial_t - \dot{x}(t_0,t)\partial_{t_0}$, where a prime stands for ∂_{t_0} and a dot for ∂_t. The subscript 2 refers to both fluids; fluid 2+ and fluid 2− are restricted to the diode region $0 \leqslant x < x_*$. In the same way, the Poisson equation (3) reads in Lagrangian coordinates for $0 \leqslant x(t_0,t) < x_\star$ as follows:

$$\ddot{x}(t_0,t) - \alpha^2\nu\,(t-t_0) + \alpha^2 \int_{t_0}^{t} d\tau\, x'(\tau,t) \sum_{+,-} \tilde{n}_2(\tau,t) = -E_0(t), \tag{12}$$

where $E_0(t) \equiv \tilde{E}(t,t)$ is the electric field at the emitter ($x = 0$). The boundary conditions are

$$x(t_0,t_0) = 0, \qquad \dot{x}(t_0,t_0) = 1, \qquad x'(t_0,t_0) = -1. \tag{13}$$

4. Equilibrium solution and stability of type I flow (no reflection)

The stationary solution with no particle reflection (type I, $\nu = 1$) can be found easily: $E_0(t) = E_0 = \text{const}$, and the quantities depend only on $q \equiv t - t_0$, reflecting the time invariance. The differentiation operators transform into

$$\partial_t \to \partial_q, \tag{14}$$

$$\partial_{t_0} \to -\partial_q, \tag{15}$$

and in the equilibrium case $\chi(q) := x(t_0,t)$ denotes the position of an electron fluid element at time t that has been injected at time t_0. Poisson's equation (12) reduces to

$$\chi''(q) - \alpha^2 q = -E_0. \tag{16}$$

Solving this ordinary differential equation and using the boundary conditions

$$\chi(0) = 0, \tag{17}$$

$$\chi'(0) = 1, \tag{18}$$

we get

$$\chi(q) = \tfrac{1}{6}\alpha^2 q^3 - \tfrac{1}{2}E_0 q^2 + q. \tag{19}$$

This solution has to satisfy three more conditions.

(a) The potential condition

$$-V = \int_0^1 E(x,t)\,dx = \int_t^{t-T} \tilde{E}(t_0,t)x'(t_0,t)\,dt_0 = -\int_t^{t-T} \ddot{x}(t_0,t)x'(t_0,t)\,dt_0 \tag{20}$$

reduces for steady-state flows to

$$-V = -\int_0^T \chi''(q)\chi'(q)\,dq \tag{21}$$

which is equivalent to the energy conservation law – both resulting in $\chi'(T) = (2V+1)^{1/2}$. In (20) and (21) the variable T denotes the transit time of an electron fluid element.

(b) The transit-time condition

$$x(t-T,t) = 1 \tag{22}$$

https://doi.org/10.1017/S0022377896004886 Published online by Cambridge University Press

transforms in the stationary case to

$$\chi(T) = 1. \tag{23}$$

(*c*) The no-return condition for fluid 1 in the case of the type I solution,

$$\dot{x}(t_0, t) \geqslant 0 \quad \text{for} \quad t_0 \leqslant t \leqslant t_0 + T, \tag{24}$$

ensures that the electron fluid never reaches negative velocities. In the steady state (24) becomes

$$\chi'(q) \geqslant 0 \quad \text{for} \quad 0 \leqslant q \leqslant T. \tag{25}$$

Equality in (24) and (25) represents the case of zero velocity at a certain position, which could be a turning point of the fluid element 1. It is given by

$$\chi'(q) = 0 \quad \Rightarrow q_{1/2} = \frac{E_0}{\alpha^2} \pm \left[\left(\frac{E_0}{\alpha^2}\right)^2 - \frac{2}{\alpha^2}\right]^{1/2}. \tag{26}$$

First, we investigate the case of a non-negative electric field at the emitter ($E_0 \geqslant 0$). $\chi'(q)$ is an open parabola with minimum value at $q_0 = E_0/\alpha^2$ and $\chi'(q_0) = -\frac{1}{2}E_0^2 + \alpha^2$. For positive electric fields, q_0 is always positive, and therefore the velocity of fluid 1 is always positive if

$$0 \leqslant E_0 < 2^{1/2}\alpha \quad \text{and} \quad 0 \leqslant q \leqslant T. \tag{27}$$

In the limiting case of $E_0 = 2^{1/2}\alpha$, for which $q_1 = q_2 = q_0 = 2^{1/2}/\alpha$ holds with $\chi'(q_0) = 0$, it is necessary for type I flow without reflection to exclude the case $0 < \chi(q_0) < 1$. This results in

$$\alpha \leqslant 2^{1/2}/3 \quad \text{for} \quad E_0 = 2^{1/2}\alpha. \tag{28}$$

For negative electric fields ($E_0 < 0$), the velocity of fluid 1 can be written as

$$\chi'(q) = \tfrac{1}{2}\alpha^2 q^2 + |E_0|q + 1, \tag{29}$$

ensuring that the velocity of fluid 1 will be always positive for negative electric fields. Therefore the region of type I solutions in the (α, E_0) plane is restricted to the right-hand side of the line $E_0 = 2^{1/2}\alpha$, including the part with $\alpha \leqslant 2^{1/2}/3$.

Physical type I solutions are further constrained by (21) and (23), leading to

$$\chi'(T) = (2V + 1)^{1/2}, \qquad \text{i.e.} \quad V \geqslant -\tfrac{1}{2}, \tag{30}$$

and to

$$\chi(T) = 1. \tag{31}$$

From the last two equations, the transit time T can be written as a function of α and V through the algebraic equation

$$-\tfrac{1}{12}\alpha^2 T^3 + \tfrac{1}{2}T[1 + (2V + 1)^{1/2}] - 1 = 0, \tag{32}$$

which has three roots. The transit time must be real and positive. It follows from this that some of the roots, being obtainable by numerical methods, can be eliminated. From (30) and (31), the electric field at the cathode E_0 can be represented as a function of T:

$$E_0 = E_0(T) = \frac{1}{T}[4 + 2\,(2V + 1)^{1/2}] - \frac{6}{T^2}. \tag{33}$$

The values of $(\alpha, E_0(\alpha, V))$ must lie in the non-hatched region of Fig. 2 in order to

https://doi.org/10.1017/S0022377896004886 Published online by Cambridge University Press

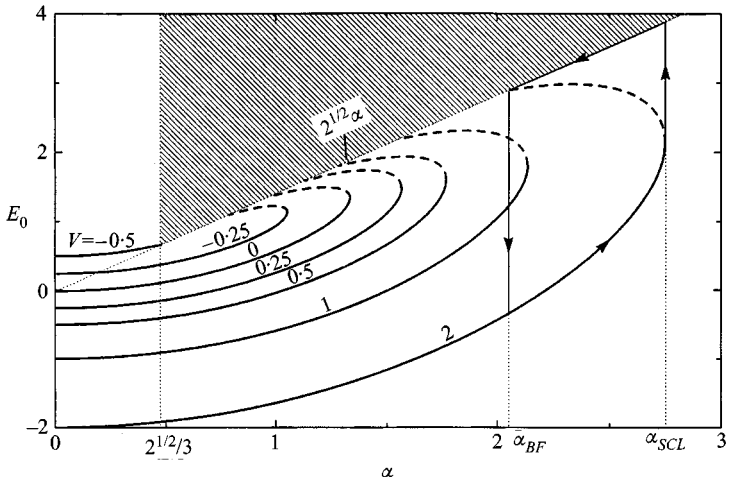


Figure 2. Existence diagram of type I flow (no reflection) in the (E_0, α) plane (where E_0 is the electric field at the emitter and α is the Pierce parameter) for different collector potentials V. For a given curve (e.g. $V = 2$), two points are of interest: the turning point α_{SCL} (space-charge limit) and the bifurcation point α_{BF}. Solid lines represent stable and dashed lines unstable branches. The latter represents the so-called C-overlap in the nomenclature of Fay *et al.*. Below $V = -0.5$, the flow experiences total reflection within the diode gap. No type I flow exists in the hatched region. For $V = 2$, a hysteresis pattern is seen: with increasing α, the solution jumps at $\alpha = \alpha_{SCL}$ to the branch with a virtual cathode given by $E_0 = 2^{1/2}\alpha$; on lowering the current, a second jump occurs at $\alpha = \alpha_{BF}$ to the stable type I flow without reflection. At $V = -0.5$ the hysteresis loop vanishes as both critical points coalesce at $2^{1/2}/3$. As $\alpha \to 0$, we observe that $E_0 \to -V$, the electric field of a capacitor free of space charges.

be a physically acceptable type I solution. Thus mathematically admissible but unphysical (because they are connected with a re-entering of the fluid element) values of $T(\alpha, V)$ can be eliminated. It can be shown that, for positive values of E_0, there always exist solutions with positive transit times, whereas solutions with a negative electric field demand a positive anode potential to get a positive T.

Alternatively, $E_0(\alpha, V)$ can also be found numerically from

$$\frac{E_0^3}{\alpha^4} \mp \left\{ \left(\frac{E_0}{\alpha^2}\right)^2 + \frac{2}{\alpha^2}[(2V+1)^{1/2} - 1] \right\}^{1/2} \left[-\frac{E_0^2}{\alpha^2} + (2V+1)^{1/2} + 2 \right] - 3\frac{E_0}{\alpha^2} + 3 = 0, \tag{34}$$

and the corresponding $T(\alpha, V)$ from

$$T_{1/2} = \frac{E_0}{\alpha^2} \pm \left\{ \left(\frac{E_0}{\alpha^2}\right)^2 + \frac{2}{\alpha^2}[(2V+1)^{1/2} - 1] \right\}^{1/2}. \tag{35}$$

Non-physical $T_{1/2}$ solutions must be excluded here too. Figures 2 and 3 show examples for the steady-state solution without particle reflection and for different potentials. The first shows the electic field at the emitter and the second the transit time as functions of α. In the notation of Fay *et al.* (1938), the lower branch is called normal C-flow and the upper branch C-overlap. The space-charge-limited flow α_{SCL} is found as a function of the anode potential V,

$$\alpha_{SCL}(V) = \tfrac{2}{3}[3V + 2 + (2V+1)^{1/2}(V+2)]^{1/2}, \tag{36}$$

https://doi.org/10.1017/S0022377896004886 Published online by Cambridge University Press

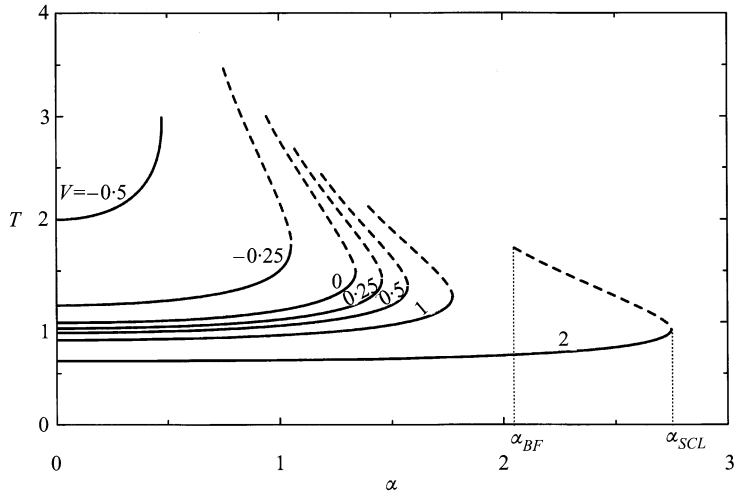


Figure 3. The transit times of type I flow as functions of α. As expected, a higher collector voltage shortens the time of flight.

and the transit time T for the space-charge limited flow is given by

$$T_{SCL}(V) = \frac{3}{1 + (2V + 1)^{1/2}}. \tag{37}$$

The corresponding electric field at the cathode can be easily determined from (33):

$$E_{0,SCL}(V) = \tfrac{2}{3}[1 + (2V + 1)^{1/2}] \tag{38}$$

The intersection of the C-overlap flow with $E_0 = 2^{1/2}\alpha$ is given by

$$\alpha_{BF}(V) = (2^{1/2}/3)[1 + (2V + 1)^{3/4}], \tag{39}$$

where the subscript BF stands for bifurcation. The corresponding value of the transit time is

$$T(\alpha_{BF}(V), V) = T_{BF}(V) = 3\,\frac{1 + (2V + 1)^{1/4}}{1 + (2V + 1)^{3/4}} \tag{40}$$

Figure 4(*a*) shows the behaviour of the two limiting values (α_{SCL}, the space-charge limit of the type I solution and α_{BF}, the minimum value of the virtual-cathode type II solution) as functions of the potential drop between the two electrodes. In Figs 4(*b*) and (*c*) the corresponding electric fields and transit times are depicted. The quantities with subscript 'cap' represent the lower boundary achieved in the limit of a diminishing electron current $\alpha \to 0$, the solution of a space-charge-free capacitor. The transit time of type I flow is always found to be shorter than that of type II flow because of the deceleration of the virtual cathode.

The stability of the two C-branches is investigated next. The differential equation describing the path of an electron fluid element through the diode (12) reduces to (no return, $\nu = 1$)

$$\ddot{x}(t_0, t) - \alpha^2(t - t_0) = -E_0(t). \tag{41}$$

The perturbation ansatz is chosen as

$$E_0(t) = E_0 + \epsilon_0 \exp(\sigma t),$$
$$x(t_0, t) = \chi(q) + y(q) \exp(\sigma t).$$

https://doi.org/10.1017/S0022377896004886 Published online by Cambridge University Press

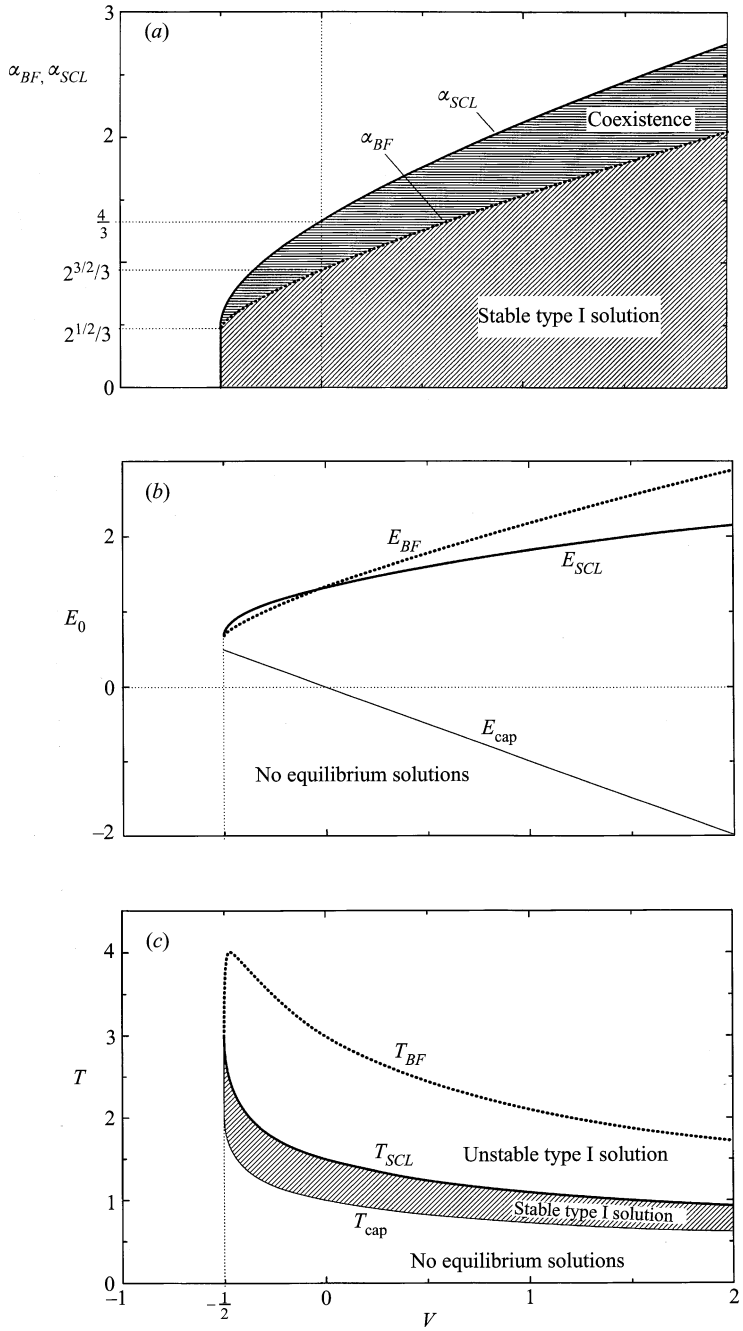


Figure 4. (*a*) The two critical points α_{BF} and α_{SCL} as functions of the collector potential V. (*b*) The three critical emitter electric fields as functions of V. $E_{\rm cap} = -V$ represents the capacitor field in the absence of space charges. Note the crossing of $E_{BF}(V)$ and $E_{SCL}(V)$ at $\frac{4}{3}$, their common value at $V = 0$. A stable type I flow exists for an E_0 ranging between $E_{\rm cap} \leqslant E_0 \leqslant E_{SCL}$. (*c*) The three critical transit times as functions of V for type I flow. $T_{\rm cap}$ denotes the transit time of a single test electron determined by the capacitor field. Stable type I solutions lie in the hatched area.

https://doi.org/10.1017/S0022377896004886 Published online by Cambridge University Press

Here E_0 and $\chi(q)$ are the familiar $O(1)$ equilibrium solutions, and the second terms are $O(\epsilon)$. Therefore at $O(\epsilon)$ one has to have

$$\sigma^2 y(q) + 2\sigma y'(q) + y''(q) = -\epsilon_0, \tag{42}$$

with the boundary conditions $y(0) = 0$, $y'(0) = 0$ and $y''(0) = -\epsilon_0$. The solution is

$$y(q) = \frac{\epsilon_0}{\sigma^2}[\exp(-\sigma q)\ (1 + \sigma q) - 1]. \tag{43}$$

This linearized solution $x(t_0, t)$ has to satisfy the potential condition (20) and the transit time condition (22) up to $O(\epsilon)$. The deviation $y(q)\exp(\sigma t)$ from the path of the equilibrium solution leads to a deviation in the transit time $T = T_0 + \delta T$ from the equilibrium value T_0. With (22), it follows that

$$\delta T = -\frac{y(T_0)}{(2V+1)^{1/2}}\exp(\sigma t). \tag{44}$$

The potential condition (20) together with (44) finally gives the dispersion relation

$$\sigma^3 - \alpha^2[(\sigma T_0 + 2)\exp(-\sigma T_0) + (\sigma T_0 - 2)] = 0, \tag{45}$$

where $T_0 = T_0(\alpha, V)$ is the transit time of the corresponding equilibrium solution. Equation (45) corresponds to the results of Lomax (1961) based on a perturbation analysis by Llewellyn (1941) starting from fluctuations in the current density. A numerical evaluation of the dispersion relation shows that the C-overlap flow is unstable (the dominant mode is purely growing), and the normal C-flow is aperiodically stable.

5. Equilibrium solution of type II flow (partial reflection)

A second type of equilibrium solution can be found within the above boundary conditions showing a partial reflection of the electron beam back to the cathode ($0 < \nu < 1$). This stationary virtual cathode solution is henceforth termed as the type II solution. Again we have $x(t_0, t) = \chi(t - t_0) = \chi(q)$, denoting the path of fluid 1 through the whole diode gap with $0 \leqslant q \leqslant T$, and $\tilde{n}_{2+}(t_0, t) = N_{2+}(q)$, $\tilde{v}_{2+}(t_0, t) = V_{2+}(q)$, $\tilde{n}_{2-}(t_0, t) = N_{2-}(q)$ and $\tilde{v}_{2-}(t_0, t) = V_{2-}(q)$ valid during the 'time' interval $0 \leqslant q < S$. S denotes the time when the injected fluid element 1 and 2+ splits into fluid 1, which crosses the diode gap, and into fluid 2−, which returns to the emitter. At $q = S$, the fluid element has reached the position of the virtual cathode, where the electric field as well as the velocity of the fluid elements vanish. At the virtual cathode, $x_* = x(t_0, t_0 + S) = \chi(S)$, the potential has a minimum and hence the electric field vanishes:

$$\tilde{E}(t_0, t_0 + S) = \mathcal{E}(S) = -\chi''(S) = 0. \tag{46}$$

A further condition reflecting zero velocity at the virtual cathode is

$$\chi'(S) = 0. \tag{47}$$

The electric field at the emitter is constant: $\mathcal{E}(0) = E_0 = -\chi''(0)$. Since in the stationary case the functions depend only on $q = t - t_0$, the differentiation operators transform as in (14) and (15) to

$$\partial_t \to \partial_q,$$
$$\partial_{t_0} \to -\partial_q,$$

https://doi.org/10.1017/S0022377896004886 Published online by Cambridge University Press

and the operator $\Xi(t, t_0)$ becomes identically 0. Therefore the continuity equations of fluids 2+ and 2−, (10), lead to

$$\partial_q[N_2(q)V_2(q)] = 0, \tag{48}$$

which can be easily integrated. Fixing the integration constants by the boundary conditions, we obtain

$$N_{2\pm}(q)V_{2\pm}(q) = \pm\tfrac{1}{2}(1-\nu). \tag{49}$$

The electron momentum equations (11), on the other hand, read

$$\partial_q\chi(q)\ \mathcal{E}(q) + \partial_q\{\tfrac{1}{2}\,[V_{2\pm}(q)]^2\} = 0. \tag{50}$$

With $\mathcal{E}(q) = -\chi''(q)$, this can be integrated, leading with (49) to

$$\chi'(q) = \frac{1-\nu}{2\,N_{2\pm}(q)}, \tag{51}$$

which is valid in the range $0 \leqslant q < S$. It determines the velocity of fluid 1 (and of fluid 2+) for $0 \leqslant x < x_*$. Singularities in the charge densities of the fluid elements are found for $q = S$, because the electron velocities become zero at the position of the virtual cathode $x_* = \chi(S)$. This can be seen from (51) or from the continuity equation of fluid 1. It is due to the cold-fluid description of the electrons. This singular behaviour is not necessarily an argument against the model: the charge density is not a quantity that is physically observable at a point, but rather only the charge in a tiny volume can be measured and this is always a finite quantity even though the charge density can be infinite at a singular point in the volume. Furthermore, in reality the injected electrons are not exactly monoenergetic but have a thermal spread in the velocity distribution (Birdsall and Bridges 1966). Poisson's equation (12) in the multistream region of the diode $0 \leqslant \chi(q) < \chi(S)$, equivalent to $0 \leqslant x < x_*$, reads

$$\chi''(q) - \alpha^2\nu q + \alpha^2\int_0^q [-\chi'(q')][N_{2+}(q') + N_{2-}(q')]\,dq' = -E_0. \tag{52}$$

With (51), it is therefore necessary to solve

$$\chi''(q) - \alpha^2 q = -E_0, \tag{53}$$

valid in the range $0 \leqslant q \leqslant S$, $0 < \chi(S) \leqslant 1$. With the usual boundary conditions $\chi(0) = 0$ and $\chi'(0) = 1$ at the cathode, it follows that

$$\chi(q) = \tfrac{1}{6}\alpha^2 q^3 - \tfrac{1}{2}E_0 q^2 + q. \tag{54}$$

At the virtual cathode (zero velocity of fluid 1, zero electric field),

$$\chi'(S) = 0, \tag{55}$$

$$\chi''(S) = 0, \tag{56}$$

leading to

$$E_0 = 2^{1/2}\alpha \tag{57}$$

$$S = \frac{2^{1/2}}{\alpha}. \tag{58}$$

A virtual cathode (type II solution) can be found for

$$\alpha \geqslant \alpha_{BF} \equiv (2^{1/2}/3)[1 + (2V+1)^{3/4}], \qquad V > -\tfrac{1}{2}, \tag{59}$$

https://doi.org/10.1017/S0022377896004886 Published online by Cambridge University Press

where the index BF stands for bifurcation (see below). Therefore in the (E_0, α) plane (Fig. 2) $E_0 = 2^{1/2}\alpha$ and $\alpha \geqslant 2^{1/2}/3$, whereby the starting point for given V is fixed by α_{BF}. For a given α with $\alpha \geqslant \alpha_{BF}$, for the type II solution, the position of the virtual cathode is fixed:

$$x_* = \chi(S) = \frac{2^{1/2}}{3\alpha}. \tag{60}$$

Note that these analytical solutions are normalized to the total electron density at the cathode, including the density of the returning electron stream 2+. This simplifies the analysis, but it is not the usual experimental situation. In an experiment it is more interesting to determine the dependences as functions of the emitted electron density n_{inj}. Accounting for this situation, we give at the end of this section the procedure for converting these results into functions of the injection density. After having passed the virtual cathode, the space charge in the region $x_* < x \leqslant 1$ is constituted by fluid 1 only, which has to satisfy (the non-integrated form) of Poisson's equation (3),

$$-\ddot{x}'(t_0, t) = \alpha^2\nu, \tag{61}$$

and in the equilibrium case

$$\chi'''(q) - \alpha^2\nu = 0. \tag{62}$$

The three boundary conditions are $\chi(S) = 2^{1/2}/3\alpha$, $\chi'(S) = 0$ and $\chi''(S) = 0$, with $S = 2^{1/2}/\alpha$ according to (58). The solution is

$$\chi(q) = \frac{1}{6}\alpha^2\nu q^3 - \frac{\alpha}{2^{1/2}}\nu q^2 + \nu q + \frac{2^{1/2}}{3\alpha}(1-\nu) \tag{63}$$

for $S \leqslant q \leqslant T$. It can be easily shown that $\chi'(q) \geqslant 0$ for $S < q \leqslant T$ and $0 < \nu < 1$. Hence no return of fluid 1 will take place in the region between the virtual cathode and the anode in the equilibrium case, which means that, under steady-state conditions, only one virtual cathode can exist in the diode gap. Type II solutions defined by (54) and (63) have to satisfy a further condition, namely the potential condition which in the stationary case is equivalent to energy conservation, leading to

$$T_{VC} = \frac{2^{1/2}}{\alpha}\left[1 + \frac{(2V+1)^{1/4}}{\nu^{1/2}}\right]. \tag{64}$$

The transit time condition (23) together with (64) fixes the splitting rate as a function of α and V:

$$\nu(\alpha, V) = \nu = \frac{(2V+1)^{3/2}}{(2^{-1/2}3\alpha - 1)^2}. \tag{65}$$

Combination of the two equations yields for the transit time T

$$T_{VC}(\alpha, V) = \frac{2^{\frac{1}{2}}}{\alpha}\left[1 + \frac{2^{-1/2}3\alpha - 1}{(2V+1)^{1/2}}\right]. \tag{66}$$

The rescaling of the control parameter α (Pierce parameter) containing the total electron density $n_0(0, t)$ at the cathode into the new control parameter β (injection parameter) containing the density of injected electrons, n_{inj} is given by

$$\beta^2 = \frac{n_{\mathrm{inj}}e^2}{\epsilon_0 m_e}\frac{L^2}{v_0^2} = \frac{n_{\mathrm{inj}}}{n_0}\alpha^2 = \frac{1+\nu}{2}\alpha^2, \tag{67}$$

https://doi.org/10.1017/S0022377896004886 Published online by Cambridge University Press

valid for stationary solutions. The injection parameter can also be expressed as a function of the incoming electron current $j_{\mathrm{inj}} = en_{\mathrm{inj}}v_0$:

$$\beta^2 = \frac{j_{\mathrm{inj}} e L^2}{\epsilon_0 m_e v_0^3}.$$

The transmitted part of the injected electron density itself has been calculated as a function of α, (65); therefore the equation

$$\beta^2 = \frac{1}{2}\left[1 + \frac{(2V+1)^{3/2}}{\left(2^{-1/2}3\alpha - 1\right)^2}\right]\alpha^2 \tag{68}$$

has to be inverted into $\alpha(\beta, V)$ in order to express all functions as functions of (β, V), which is more convenient for comparison with the experiment. The type I solution is obviously contained as a special case ($\nu = 1$, $\alpha = \beta$) in the general case of partial reflection. The bifurcation point α_{BF}, where the transistion from the type I to the type II flow takes place, coincides with β_{BF} as expected. One way to get the rescaling laws from (68) is the following. For a type II solution, $\alpha \geqslant \alpha_{BF} = (2^{1/2}/3)[1 + (2V+1)^{3/4}]$ and $V > -\frac{1}{2}$, (59). The dependence of the position of the virtual cathode x_* on α, namely $x_* = 2^{1/2}/3\alpha$, can be used for the definition of a new quantity $y_* \equiv (1/x_*)^2$. Equation (68) then becomes

$$(3\beta)^2 = y_*\left[1 + \frac{C}{(y_*^{1/2} - 1)^2}\right] \tag{69}$$

with $C = (2V+1)^{3/2}$. The next step consists in solving this equation with respect to y_* with an analytical mathematical program such as MAPLE V (Char *et al.* 1991), yielding four roots, whereby the sought solution must satisfy

$$0 = \beta_{BF} - \alpha_{BF} = \beta_{BF} - (2^{1/2}/3)\left[y_*(\beta_{BF})\right]^{1/2}. \tag{70}$$

Through this equation, two of the solutions can be eliminated. A second boundary condition for fixing the solution will be used later. Finally, the proper root $y_* = y_*(\beta, V)$ is determined, giving the position of the virtual cathode as

$$x_*(\beta, V) = \left[y_*(\beta, V)\right]^{-1/2}. \tag{71}$$

Now, more interesting quantities for the type II solutions can be calculated as functions of β, and thus indirectly as functions of the injection current j_{inj}. For example, $\alpha(\beta)$ is given by

$$\alpha(\beta, V) = (2^{1/2}/3)\left[y_*(\beta, V)\right]^{1/2}. \tag{72}$$

Now $[y_*(\beta, V)]^{1/2}$ can be written down explicitly as

$$[y_*(\beta, V)]^{1/2} = \frac{1}{6}\left\{3 + d_1^{1/2} \pm \left[2c_1 - c_2 - c_3 - 54\frac{(C + 9\beta^2)}{d_1^{1/2}}\right]^{1/2}\right\}, \tag{73}$$

with

$$\begin{aligned} d_1 &:= c_1 + c_2 + c_3, \\ c_1 &:= -6\mathcal{C} + 9, \qquad c_2 := 9b^{1/3}, \qquad c_3 := \mathcal{C}^2 b^{-1/3}, \\ b &:= a_1 + \tfrac{2}{3}a_2^{1/2}, \end{aligned}$$

https://doi.org/10.1017/S0022377896004886 Published online by Cambridge University Press

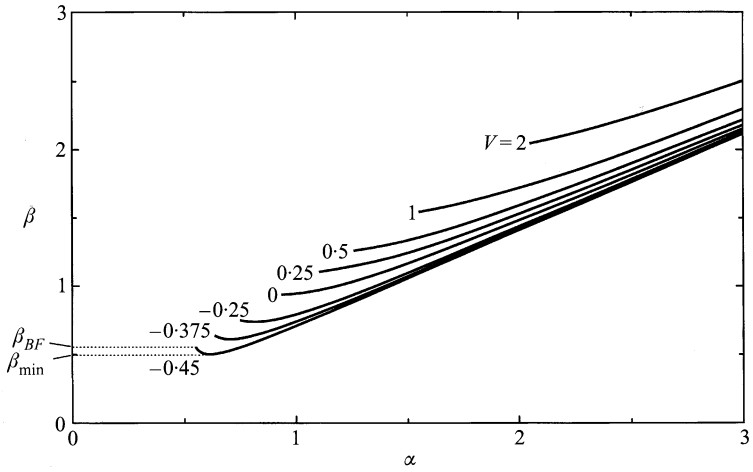


Figure 5. The injection parameter β as function of the Pierce parameter α for different values of V. For negative potentials, the slope undergoes a zero transition. This implies two choices of α for a given β: $\beta_{\min} \leqslant \beta \leqslant \beta_{BF}$.

$$a_1 := \tfrac{1}{27}\,\mathcal{C}^3 + 18C\beta^2, \qquad a_2 := 3C\beta^2\left(\mathcal{C}^3 + 243C\beta^2\right),$$
$$\mathcal{C} := C + 1 - 9\beta^2, \qquad C := (2V+1)^{3/2}.$$

Some of these quantities can become complex. However, $[y_*(\beta, V)]^{1/2}$ is real. The more interesting point is the $\pm$ in (73), accounting for a branch cut. The signs are found as follows. First, the diagram resulting from (68), namely showing β as a function of α for different potentials V for the type II or virtual cathode solution, is drawn (Fig. 5). For negative potentials, a minimum value $\beta_{\min}$ smaller than $\beta_{BF} = \alpha_{BF}$ can be found, given by

$$\beta_{\min} = \tfrac{1}{3}(1 + C^{1/3})^{3/2}, \tag{74}$$
$$\alpha(\beta_{\min}) = (2^{1/2}/3)(1 + C^{1/3}), \tag{75}$$
$$\nu(\beta_{\min}) = C^{1/3}. \tag{76}$$

As can be seen from (74) and (70), the minimum value $\beta_{\min}$ is smaller than $\beta_{BF} = \alpha_{BF}$. This leads to interesting conclusions: for negative anode potentials, virtual cathode solutions can be found for injection currents β greater than $\beta_{\min}$. For such βs (greater than $\beta_{\min}$ and smaller than β_{BF}), there exist two possibilities for the splitting rate ν and therefore two possibilities for α, which is normalized to the total electron density at the emitter. The smaller value of α is found by taking the minus sign in (73), and the corresponding larger value by taking the plus sign. This can be verified as follows. For a given ν in the range $0 < \nu < 1$, the correct branch has to satisfy

$$\beta_\nu = [\tfrac{1}{2}(1+\nu)]^{1/2}\alpha_\nu. \tag{77}$$

Thus α_ν can be calculated directly from (65) as a function of the potential for a given ν:

$$\alpha_\nu = \frac{2^{1/2}}{3}\left(1 + \frac{C^{1/2}}{\nu^{1/2}}\right). \tag{78}$$

Furthermore, the right-hand side of (72) must coincide with α_ν from (78). A close

https://doi.org/10.1017/S0022377896004886 Published online by Cambridge University Press

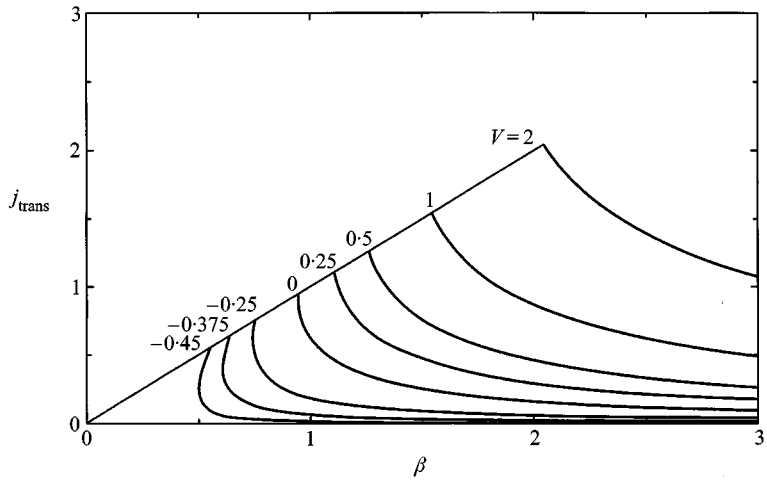


Figure 6. The transmitted current j_{trans} as a function of β for various values of V.

look at the numerically evaluated α_νs as functions of C and for the two different signs in $[y_*(\beta_\nu)]^{1/2}$ in (73) confirms the right choice of the sign.

Now, one remaining interesting quantity, namely the portion of transmitted current, can be determined. The transmitted current normalized to the injection current is given by the ratio

$$\eta(\beta, V) = \frac{\nu(\beta, V)}{n_{\text{inj}}/n_0} = \frac{2\,\nu(\beta, V)}{\nu(\beta, V) + 1}, \tag{79a}$$

with

$$\nu(\beta, V) = \frac{(2V+1)^{3/2}}{\{[y_*(\beta, V)]^{1/2} - 1\}^2}. \tag{79b}$$

Figure 6 shows the transmitted current $j_{\text{trans}} = \beta\,\eta(\beta, V)$ as a function of the injected electron current β. For completeness, two diagrams (Figs 7 and 8) are given showing the electric field E_0 and the transit time T as functions of β for the type II flow. From Fig. 7, we see that, for a given V, $E_0(\beta)$ is no longer a strictly linear function of the control parameter β, in contrast to $E_0(\alpha)$ (Fig. 2), as can be expected from the nonlinear relation $\beta = \beta(\alpha)$ shown in Fig. 5. There is an asymptote $E_{0,\text{as}} = 2\beta$ above which no type II solutions exist. This upper branch is in accordance with the work of Kuznetsov *et al.* (1994), who found $2^{1/2} \leqslant \epsilon_0 \equiv E_0/\beta < 2$. From Fig. 8, which shows the transit times of type II flows as functions of β for various values of V, we see a remarkable quantitative increase in the transit time T with decreasing V. In the short-circuited diode ($V = 0$) the transit time is independent on the injection current. The transit time T decreases (increases) as a function of β with increasing (decreasing) potential. The hysteresis shown in Fig. 2 is depicted now in terms of the injection current β in Fig. 9. Here the values of the electric potential E_0 at the emitter are shown for when the injection parameter is raised or lowered quasistatically at $V = 2$.

Figure 10 shows the position x_* of the virtual cathode as a function of the injected current for different values of the potential. An increase in β shifts x_* closer to the emitter for $V \geqslant 0$. Figure 11 depicts the minimum potential in the diode as

https://doi.org/10.1017/S0022377896004886 Published online by Cambridge University Press

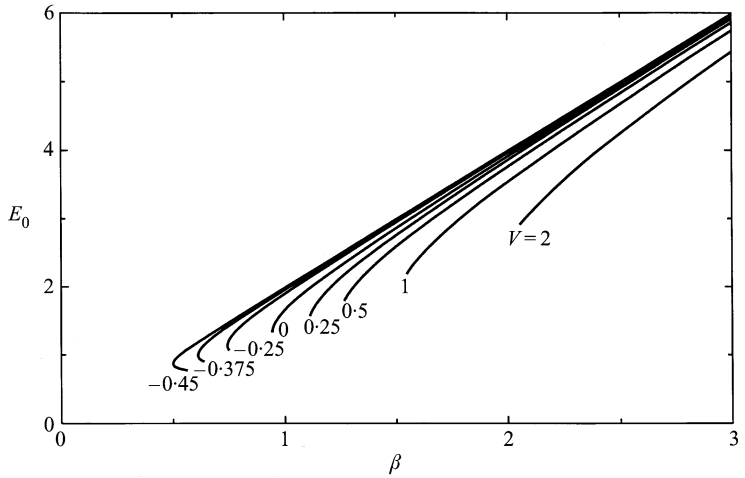


Figure 7. The electric field at the emitter, E_0, as function of the injection parameter β for various values of the collector potential V.

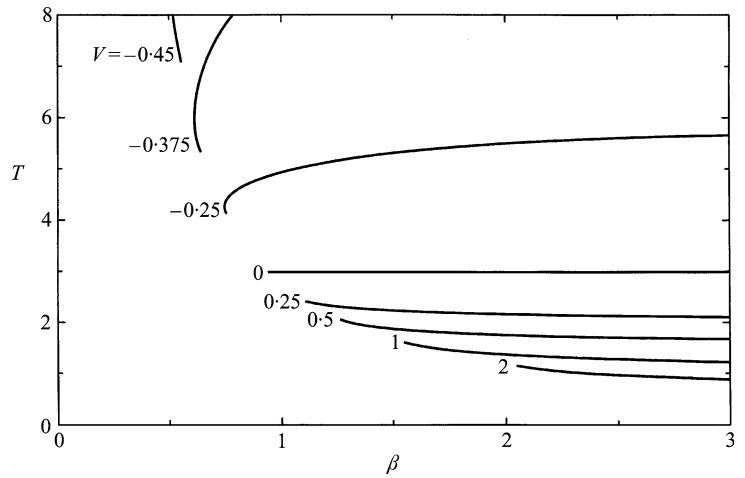


Figure 8. The transit time for type II flow as function of the injection parameter β for various values of the collector potential V.

a function of the injection current. The horizontal line at $\Phi_{\min} = -\frac{1}{2}$ represents type II flow with partial reflection of electrons, the curved lines are for type I flow with no electron reflection. Dashed lines correspond to unstable solutions. Similar diagrams have been presented for the short-circuited case by Coutsias and Sullivan (1983) and Kuznetsov *et al.* (1994). For the type I flow, we find using (16), with $E(q_*) = -\chi''(q_*) = 0$, from energy conservation and from (19),

$$\Phi_{\min} = \frac{1}{2}\left(\frac{E_0}{\beta}\right)^2\left[\left(\frac{E_0}{2\beta}\right)^2 - 1\right]. \tag{80}$$

Let us search for the β range where this formula is valid. The time of flight is given by $q_* = E_0/\beta^2$, which must satisfy $0 < q_* \leqslant T$. For negative collector potentials and small β values, the calculated potential minimum will be found beyond the

https://doi.org/10.1017/S0022377896004886 Published online by Cambridge University Press

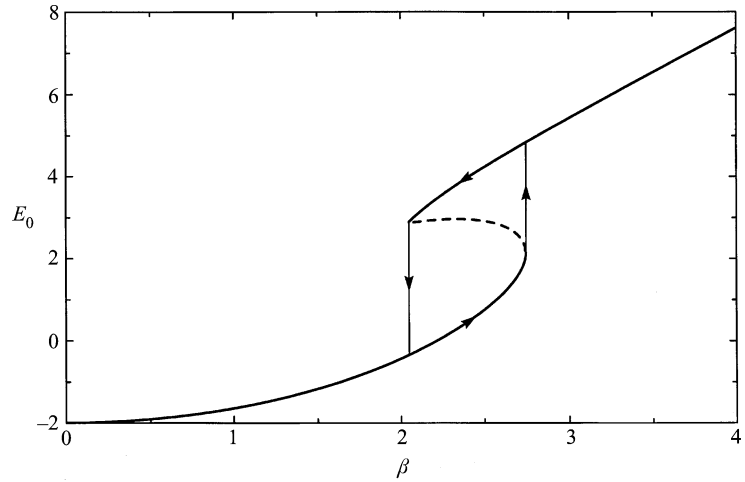


Figure 9. The hysteresis already seen from Fig. 2 is now depicted as function of the injection parameter β for $V = 2$.

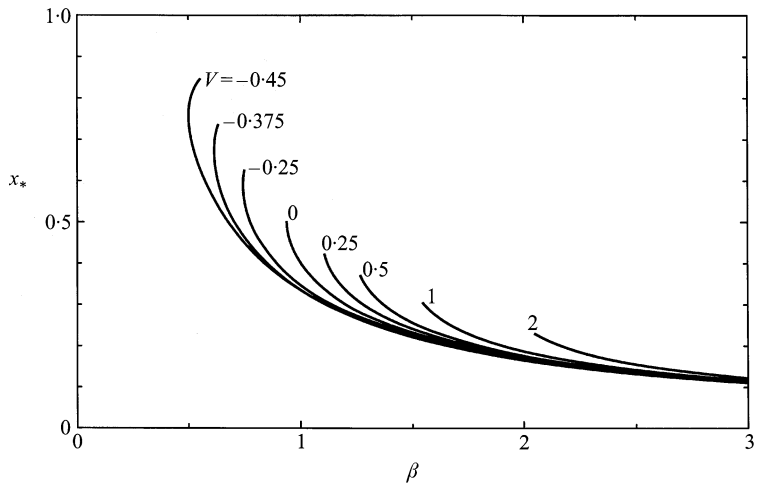


Figure 10. The position of the virtual cathode as function of the injection parameter β for various values of the collector potential V.

collector grid. Therefore, for $0 < \beta < \beta_0$, the corresponding potential profile in the diode gap is monotonically decreasing and the corresponding potential minimum is given by $\Phi_{\min} = V$ and

$$0 < \beta \leqslant \beta_0(V) = (2^{1/2}/3)[1 + 2(2V + 1)^{1/2}][1 - (2V + 1)^{1/2}]^{1/2}, \tag{81a}$$

$$-\tfrac{1}{2} < V < 0. \tag{81b}$$

For positive potentials and negative electric fields at the emitter, stricly monotonically growing potential profiles inside the diode gap are found provided that

$$0 < \beta \leqslant \beta_1(V) = (2^{1/2}/3)[2 + (2V + 1)^{1/2}][(2V + 1)^{1/2} - 1]^{1/2}, \tag{82a}$$

$$V > 0. \tag{82b}$$

https://doi.org/10.1017/S0022377896004886 Published online by Cambridge University Press

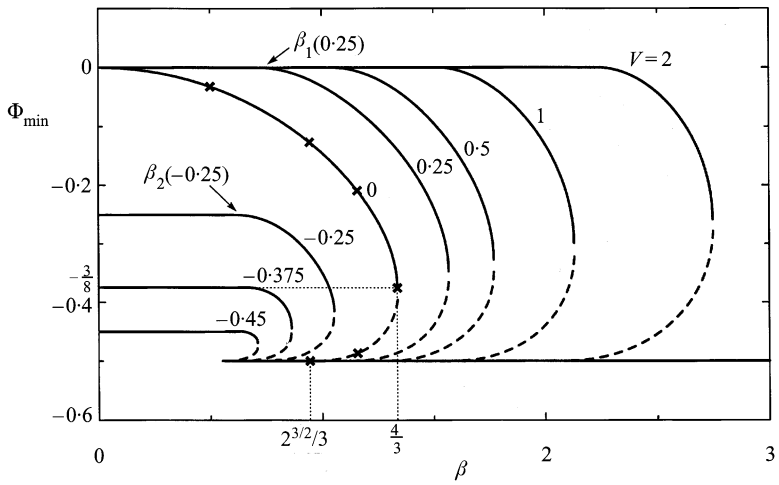


Figure 11. The potential minimum within in the diode gap as function of the injection parameter β for various values of the collector potential V. The curve for $V = 0$ coincides with that of Kuznetsov *et al.* (1994). Some points from their figure 1 are shown by crosses. For positive potentials and small injection currents ($\beta < \beta_1$), the potential profile inside the diode is monotonically increasing. For negative voltages ($-\frac{1}{2} < V < 0$), a monotonically decreasing potential profile is found for $\beta < \beta_0$. Therefore the value of the potential minimum is either the emitter or the collector potential.

Therefore the potential minimum in this case is given by $\Phi_{\min} = 0$. The depth of the potential minimum for the bifurcation point $\beta_{BF} = \alpha_{BF}$ is $\Phi_{\min} = -\frac{1}{2}$, and the minimal potential value for the space-charge limit ($\beta_{SCL} = \alpha_{SCL}$) is given by

$$\Phi_{\min,SCL} = -\frac{1}{2}\frac{6 + 16V + 9V^2 + 2(2V+1)^{1/2}(3 + 5V + V^2)^2}{[3V + 2 + (2V+1)^{1/2}(V+2)]^2}. \tag{83}$$

The position of the potential minimum for type I flows can easily be calcultated from (19). The coincidence of our analytical results with the numerical ones of Kuznetsov *et al.* (1994) represented by crosses is shown for $V = 0$ in Fig. 11.

6. Summary and conclusions

In this paper the classical problem of electron flow configurations in pure electron diodes has been revisited. A Lagrangian formalism has been adopted for two possible DC states, namely flow without (type I) and with partial reflections (type II). As a result, analytical expressions for the transmitted current, the electric field at the emitter, the transit time of transmitted particles, the virtual cathode position and the splitting rate have been obtained in terms of the injected current and of the potential drop, and these generalize earlier results. They render possible an analytical description for arbitrary potential drops of the hysteresis characterized by the two transitions between type I and type II flows, namely when the injection current exceeds the space-charge-limited current and when it falls below the bifurcation current, respectively.

A challenge, however, remains to be attacked, namely the virtual cathode oscillations as they are observed numerically and experimentally. A perturbation in the virtual cathode introduces a feedback between reflected and incoming fluid elements, which destabilizes the DC state of type II flows and introduces a stable limit

https://doi.org/10.1017/S0022377896004886 Published online by Cambridge University Press

cycle. Whether analytical progress can be achieved in this direction is, however, an open question. First steps were made, for example, by Sullivan *et al.* (1987), Thode (1987), Kadish *et al.* (1986) and Jiang *et al.* (1995).

With respect to thermionic energy conversion (TEC) (Hatsopoulus and Gyftopoulus 1973, 1979; Rasor 1991), it seems desirable to extend the above analysis of the unneutralized electron beam to beams with an arbitrary neutralization ratio ($\gamma = n_i/n_e$) for classifying the flows in a simplified model for the TEC (A. Ya. Ender, personal communications 1995).

Acknowledgements

We thank Andrey Ya. Ender for the stimulating discussions during his visit to Bayreuth University. We thank him and his colleague V. I. Kuznetsov for pointing out an error in an earlier version of Fig. 11 as well as for further discussions on the Bursian diode problem.

References

Birdsall, C. K. & Bridges, W. B. 1966 *Electron Dynamics of Diode Regions*. Academic Press, New York.

Char, B. C., Geddes, K. O., Gonnet, G. H., Leong, B. L., Monagan, M. B. & Watt, S. M. 1991 *MAPLE V Library Reference Manual*. Waterloo Maple Software.

Child, C. D. 1911 *Phys. Rev., Ser. I* **32**, 492.

Coutsias, E. A. & Sullivan, D. J. 1983 *Phys. Rev.* **A27**, 1535.

Crystal, T. L. & Kuhn, S. 1985 *Phys. Fluids* **28**, 2116.

Dunn, D. A. & Ho, I. T. 1963 *AIAA J.* **1**, 2770.

Farouki, R. T., Dalvie, M. & Pavarino, L. F. 1990 *J. Appl. Phys.* **68**, 6106.

Fay, C. E., Samuel, A. L. & Shockley, W. 1938 *Bell Syst. Tech. J.* **17**, 49.

Gill, E. W. B. 1925 *Phil. Mag.* **49**, 993.

Godfrey, B. B. 1987 *Phys. Fluids* **30**, 1553.

Harries, J. H. O. 1936*a* *Wireless Engineer* **13**, 190.

Harries, J. H. O. 1936*b* *Television Soc.* **2**, 106.

Hatsopoulus, G. N. & Gyftopoulus, E. P. 1973 *Thermionic Energy Conversion,* Vol. I. *Processes and Devices*. MIT Press, Cambridge, MA.

Hatsopoulus, G. N. & Gyftopoulus, E. P. 1979 *Thermionic Energy Conversion,* Vol. II. *Theory, Technology, and Application*. MIT Press, Cambridge, MA.

Hörhager, M. & Kuhn, S. 1990 *Phys. Fluids* **B2**, 2741.

Jiang, W., Masugata, K. & Yatsui, K. 1995 *Phys. Plasmas* **2**, 982.

Kadish, A., Faehl, R. J. & Snell, C. M. 1986 *Phys. Fluids*, **29**, 4192.

Kolinsky, H. & Schamel, H. 1994 *Phys. Plasmas* **1**, 2359.

Kolinsky, H. & Schamel, H. 1995 *Phys. Rev.* **E52**, 4267.

Kuznetsov, V. I., Solov'ev, A. V. & Ender, A. Ya. 1994, *Zh. Tekh. Fiz.* **64**, 9 [*Soviet Phys. Tech. Phys.* **39**, 1207].

Langmuir, I. 1923 *Phys. Rev.* **21**, 419.

Lawson, W. S. 1989*a* *Phys. Fluids* **B1**, 1483.

Lawson, W. S. 1989*b* *Phys. Fluids* **B1**, 1493.

Lieberman, M .A. & Lichtenberg, A. J. 1994 *Principles of Plasma Discharges and Materials Processing*. Wiley, New York.

Llewellyn, F. B. 1941 *Electron Inertia Effects*. Cambridge University Press.

Lomax, R. J. 1961 *Proc. IEE, Pt C* **108**, 119.

Pierce, J. R. 1944 *J. Appl. Phys.* **15**, 72.

Rasor, N. S. 1991 *IEEE Trans. Plasma Sci.* **19**, 1191.

Salzberg, B & Haeff, A. V. 1938 *RCA Rev.* **2**, 336.

https://doi.org/10.1017/S0022377896004886 Published online by Cambridge University Press

Schamel, H. & Bujarbarua, S. 1993 *Phys. Fluids* **B5**, 2278.

Schamel, H. & Maslov, V. 1993 *Phys. Rev. Lett.* **70**, 1105.

Strutt, M. J. O. & van der Ziel, A. 1938 *Physica* **5**, 705.

Sullivan, D. J., Walsh, J. E. & Coutsias, E. A. 1987 *High-Power Microwave Sources* (ed. V. L. Granatstein & I. Alexeff), pp. 441–505. Artech House, Norwood, MA.

Thode, L. E. 1987 *High-Power Microwave Sources* (ed. V. L. Granatstein & I. Alexeff), pp. 507–562. Artech House, Norwood, MA.

https://doi.org/10.1017/S0022377896004886 Published online by Cambridge University Press